Advances in Radiation Oncology (2025) **10**, 101904

advances in radiation oncology

www.advancesradonc.org

Scientific Article

A Precise Reirradiation Supporting Tool Initiative (PRISTIN) for Prescribing Absorbed Dose and Number of Fractions in Reirradiation

Mayu Hagiwara, MS,[a] Ryusuke Suzuki, PhD,[a,b] Seishin Takao, PhD,[b] Rumiko Kinoshita, MD, PhD,[c] Shizusa Yamazaki, MS,[a] Keiji Nakazato, MS,[b] Hideki Kojima, MP,[d] Takayuki Hashimoto, MD, PhD,[e] Keiji Kobashi, PhD,[e] Yasuhiro Onodera, PhD,[e] Hisanori Fukunaga, MD, PhD,[f] Hidefumi Aoyama, MD, PhD,[g] Michael F Gensheimer, MD,[h] Masahiro Mizuta, PhD,[i] and Hiroki Shirato, MD, PhD[e,*]

[a]Graduate School of Biomedical Science and Engineering, Hokkaido University, Sapporo, Japan; [b]Department of Medical Physics, Hokkaido University Hospital, Sapporo, Japan; [c]Department of Radiation Oncology, Hokkaido University Hospital, Sapporo, Japan; [d]Department of Radiation Oncology, Sapporo Higashi Tokushukai Hospital, Sapporo, Japan; [e]Global Center for Biomedical Science and Engineering, Faculty of Medicine, Hokkaido University, Sapporo, Japan; [f]Department of Biomedical Science and Engineering, Faculty of Health Sciences, Hokkaido University, Sapporo, Japan; [g]Department of Radiation Oncology, Faculty of Medicine, Hokkaido University, Sapporo, Japan; [h]Department of Radiation Oncology, School of Medicine, Stanford University, Stanford, CA, United States; and [i]The Institute of Statistical Mathematics, Tachikawa, Japan

Received 28 May 2025; accepted 4 September 2025

Purpose: This study aims to develop a supporting tool to calculate the most appropriate prescribing absorbed dose and number of fractions for precise reirradiation.

Methods and Materials: After deformable image registration of the initial computed tomography to the computed tomography at reirradiation, an initial biological effective dose (BED) taking into account the recovery from the initial irradiation is calculated voxel-by-voxel for each organ at risk (OAR). Using a commercial radiation therapy planning system, the clinical target volume for reirradiation (CTV2) is made. Keeping the $BED_{\text{tumor's }\alpha/\beta}$ to CTV2, cumulative $BED_{\text{OAR's }\alpha/\beta}$($CBED_{\text{OAR's }\alpha/\beta}$) in each voxel of critical OARs is calculated by changing the number of fractions in a stepwise process. The most appropriate prescribing absorbed dose to the target and the number of fractions in reirradiation is determined by using $CBED_{\text{OAR's }\alpha/\beta}$-volume histogram for critical OARs. The function of the tool was validated in silico using 3 scenarios in 2 patients: a patient with a lung cancer at the peripheral lung parenchyma and at the hilar lymphatic region at different times, and in a patient with a metastatic internal mammary lymph node relapsed after postoperative radiation therapy for breast cancer.

Results: In scenario 1, giving 57 Gy in 22 fractions (57 Gy/22 Fr) to the CTV2 at the right hilum, the maximum $CBED_{\alpha/\beta=2}$ was 124.078 Gy, and the mean $CBED_{\alpha/\beta=2}$ of the whole lung parenchyma excluding gross tumor volume was 18.332 Gy. In scenario 2, 44.152 Gy/7 Fr to the target was suggested to be most appropriate. In scenario 3, 71.675 Gy/30 Fr proton therapy to the target was

Sources of support: This work was supported by JSPS KAKENHI (19H03591, 24K10903).
All data discussed during this study are included in this published article.
*Corresponding author: Hiroki Shirato, MD, PhD; Email: shirato@med.hokudai.ac.jp

https://doi.org/10.1016/j.adro.2025.101904

recommended in which the maximum $CBED_{\alpha/\beta=2}$ in the aorta near the recurrence site was 145.796 Gy, and the volume of $CBED_{\alpha/\beta=2} \geq$ 100 Gy was 0.800 cm^3, both are within the constraints.

Conclusions: The tool was suggested to be useful to find the most appropriate prescribing absorbed dose to the target as well as the number of fractions for precise reirradiation.

Introduction

The number of patients who receive radiation therapy (RT) twice or more is increasing.[1-7] Precise reirradiation (PRI), in which prescribing absorbed dose to the target, number of fractions, and 3-dimensional (3D) dose distribution are precisely determined and delivered with sophisticated image guidance, is a big issue nowadays.[8,9] Considering the high risk of serious adverse effects of reirradiation,[10] careful assessment of cumulative dose, usage of an appropriate number of fractions is mandatory.[8,11] Also, a new external beam RT technology, such as proton therapy, is increasingly used for reirradiation.[12,13]

However, there are still problems with how to use the cumulative dose assessment in reirradiation.[14] Hypofractionated schedule is often used in initial RT using stereotactic body RT (SBRT) and image-guided RT. Late adverse effect of each organ at risk (OAR) depends at least on the tissue structure (parallel-type or serial-type), prescribing absorbed dose, number of fractions, 3D dose distribution, type of radiation beam (photon, proton), and the time from the initial RT. Rapid assessment of the biological effect of initial RT in medical physics consultation is critical to perform PRI.[15] In PRI, therefore, biological assumptions need to be the state-of-the-art concept, open to reassessment as more information becomes available, and robust enough to be accepted by radiation oncologists and medical physicists.

Recently, voxel-by-voxel calculation of accumulated equieffective dose at 2-Gy per fraction (EQD2) or biological effective dose (BED) with organ-specific α/β and recovery factor in the treatment planning was reported to be the top priority to be developed for PRI.[16] Accordingly, voxel-by-voxel accumulated EQD2 estimation function for reirradiation with a commercial 3D RT planning system (3DRTP) is increasingly reported.[17-19] These tools have achieved important solutions for PRI, but seem not to have a function to select the appropriate number of fractions. It would be useful if a supporting tool for PRI could output the appropriate number of fractions without violating institutional protocols.

Previous studies have shown that the optimal number of fractions can be recommended based on the absorbed dose distribution and the difference in α/β ratios in a linear-quadratic model between tumor and late-responding tissues.[20-24] According to these studies, for example, a solitary lung cancer in peripheral lung is to be treated in hypofractionation, but a hilar lymphatic area of lung is to be treated in multiple fractionations if the damage to the serial OAR, such as main bronchus is concerted.[20] Recently, we have developed an in-house treatment planning support software tool for PRI in which the number of fractions as well as prescribing absorbed dose can be selected based on absorbed dose distribution, tissue structure, and α/β ratios for tumor and late-responding tissues in the linear-quadratic model. The treatment planning support software tool for PRI is versatile, has a high degree of freedom to suit the objectives of each research group. In this study, we describe the PRI supporting tool and apply it to 3 clinical scenarios to investigate whether the tool is useful in PRI. We call the software Precise Re-Irradiation Supporting Tool INitiative (PRISTIN) (PRI supporting tool initiative) in this manuscript.

Methods and Materials

Flowchart

Flowchart is shown in Fig. 1. We have used software for deformable image registration (DIR), 3DRTP commercially available, and PRISTIN. The software PRISTIN consists of PRISTIN-1 and PRISTIN-2. In the workflow, (1) DIR, (2) PRISTIN-1, (3) 3DRTP, and (4) PRISTIN-2 are used sequentially in this order.

Deformable image registration

The initial CT for initial RT (first CT) is modified to conform to the CT for reirradiation (second CT) (Supplementary E1A).

Precise Reirradiation Supporting Tool Initiative-1

Initial biological effective dose ($iBED_{OAR's\ \alpha/\beta}$) after correction for recovery of occult radiation injury in each voxel in the critical OARs is calculated, using Digital Imaging and Communications in Medicine-RadioTherapy data (RT image, RT dose, RT structure, RT plan) of the first plan, taking into account the recovery from the start of initial irradiation to the start of reirradiation (Supplementary E2). We call this part of PRISTIN-1 (Supplementary E1B).

Three-dimensional radiation therapy planning system

A draft of treatment planning for reirradiation is made giving sufficient absorbed dose to the clinical target

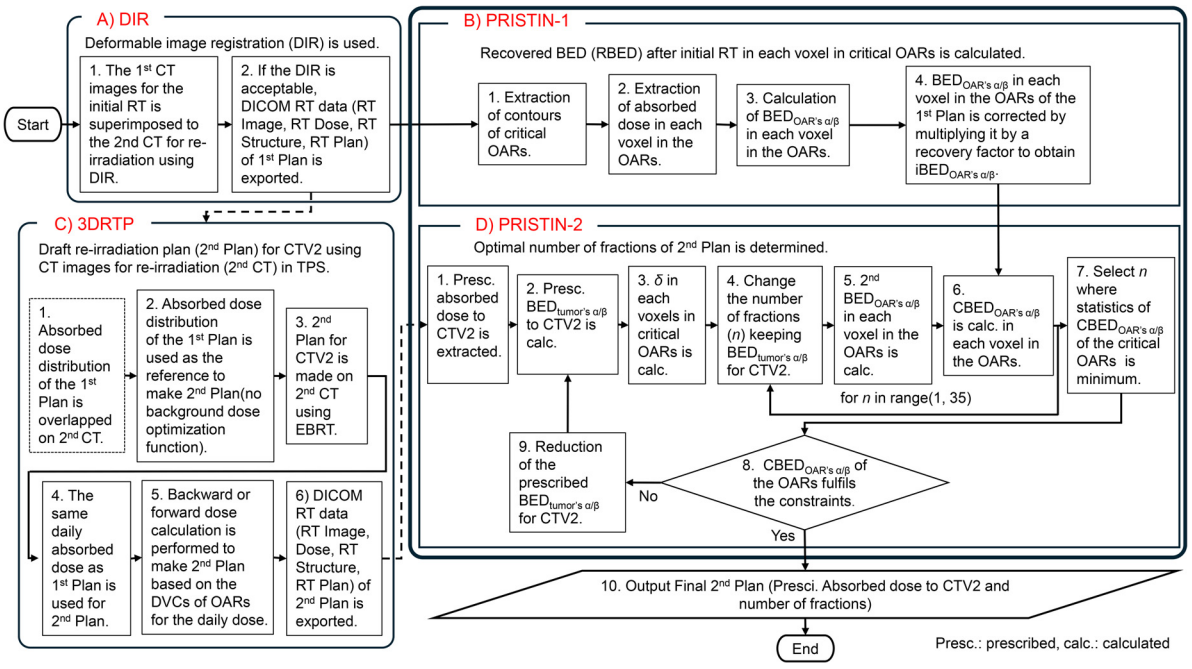

Figure 1 Flowchart for prescribing absorbed dose and number of fractions in reirradiation.
Abbreviations: 3DRTP = 3-dimensional radiation therapy planning system; CT = computed tomography; BED = biological effective dose; CBED = cumulative BED; DICOM = digital imaging and communications in medicine; DVC = dose-volume constraints; EBRT = external beam radiation therapy; RT = radiation therapy; TPS = treatment planning system; OAR = organ at risk. [δ]The normalized total absorbed dose, the ratio dividing the absorbed dose in each voxel by the prescribing total absorbed dose to the reference point of clinical target volume (CTV).

volume for reirradiation (CTV2), whether by inverse or forward calculation using 3DRTP commercially available. The same daily absorbed dose as the initial RT is often applied here to use the dose-volume constraints same as the initial RT. We call this draft plan for reirradiation as second plan in this study. On the other hand, the final plan for reirradiation is called as final second plan explicitly in this study (Supplementary E1C).

PRISTIN-2 (Supplementary E1 and E2)

Using the Digital Imaging and Communications in Medicine-RadioTherapy data of second plan, $BED_{tumor's\ \alpha/\beta}$ for CTV2 in second plan, $2ndBED_{tumor's\ \alpha/\beta}$, is calculated. Keeping the $2ndBED_{tumor's\ \alpha/\beta}$ as the prescribing $BED_{tumor's\ \alpha/\beta}$ for CTV2, number of fractions n is changed. The normalized total absorbed dose δ, the ratio dividing the absorbed dose in each voxel by prescribing total absorbed dose to the reference point of CTV2, is calculated. For each n, $BED_{OAR's\ \alpha/\beta}$ of each voxel in the OAR (2nd $BED_{OAR's\ \alpha/\beta}$) is calculated using δ in each voxel. For each n, $CBED_{OAR's\ \alpha/\beta}$, which is $iBED_{OAR's\ \alpha/\beta}$ plus 2nd $BED_{OAR's\ \alpha/\beta}$, of each voxel in the OAR is calculated sequentially. Optimal number of fractions is determined based on the distribution of $CBED_{OAR's\ \alpha/\beta}$ in critical OARs keeping the same $2ndBED_{tumor's\ \alpha/\beta}$.[20,21] In our method, we determine the allowable prescribing absorbed dose and number of fractions for reirradiation by minimizing the most relevant CBED statistic for OAR: the maximum CBED for serial organs and the mean CBED for parallel organs. This approach ensures that the tissue tolerance is respected for each OAR type, and the final second plan is selected when these minimum values are achieved, thereby prioritizing patient safety and organ preservation. When the statistics of the $CBED_{OAR's\ \alpha/\beta}$ for critical OARs are the best, that is, when the maximum $CBED_{OAR's\ \alpha/\beta}$ in serial OARs or the mean $CBED_{OAR's\ \alpha/\beta}$ in parallel OARs is minimum (Supplementary E3), PRISTIN outputs the final second plan. The final second plan shows the most appropriate set of the prescribing absorbed dose and the number of fractions to the CTV2 at the same $BED_{tumor's\ \alpha/\beta}$ to the CTV2. Final second plan is selected by iterative calculation when physician wants to try higher or lower $BED_{tumor's\ \alpha/\beta}$. Example of the stepwise process is shown in the next section.

Example of stepwise process to determine the number of fractions

α/β value in linear-quadratic model is assumed to be 10.0 for tumor and 2.0 for any late effects of OARs, respectively, in this study for simplicity because tumors generally exhibit less sensitivity to fraction size (higher α/β), while late-responding normal tissues are much more sensitive (lower α/β), as supported by extensive radiobiological and clinical studies.[25,26] Relative biological effectiveness was assumed to be 1.1 constantly and relative

biological effectiveness -weighted dose was used in proton therapy instead of absorbed dose.

(1) Other biological assumptions are shown in Supplementary E2.
(2) In this study, n was changed from 1 to 35 as an example.
(3) The max BED $_{\text{OAR's }\alpha/\beta}$ to serial OARs and the mean BED $_{\text{OAR's }\alpha/\beta}$ to parallel OARs are calculated for each number of fractions and tabulated from n = 1 to 35 (Supplementary E4 as an example).
(4) The minimum and the maximum number of fractions, weekly frequency of treatment, and the maximum treatment period for the patient are predetermined by institutional protocols considering the pathologic type of the cancer, size of the target, and uncertainties behind the biological models assumed by the institution.
(5) Based on the institutional minimum and the maximum number of fractions, the n for final second plan is selected when the statistics of the $\text{CBED}_{\text{OAR's }\alpha/\beta}$ for critical OARs are the best, that is, when the maximum $\text{CBED}_{\text{OAR's }\alpha/\beta}$ in serial OARs or the mean $\text{CBED}_{\text{OAR's }\alpha/\beta}$ in parallel OARs is minimum.
(6) If the intended $\text{2ndBED}_{\text{tumor's }\alpha/\beta}$ for the CTV2 violates $\text{BED}_{\text{OAR's }\alpha/\beta}$-volume constraints of critical OARs using any number of fractions, the prescribing absorbed dose to CTV2 is reduced (Supplementary E2).
(7) If the physician wants to increase the $\text{2ndBED}_{\text{tumor's }\alpha/\beta}$, the prescribing absorbed dose to CTV2 is increased as long as $\text{CBED}_{\text{OAR's }\alpha/\beta}$ to critical OARs is not exceeding thresholds.

In-silico simulation study in 3 scenarios

We have evaluated the usefulness of the PRISTIN in 3 scenarios, which are classified as type 1(overlap of irradiated volumes) or type 2 (concern for toxicity from cumulative doses) in the classification proposed by the European Society for Radiotherapy and Oncology and the European Organization for Research and Treatment of Cancer.[8] Usage of the medical information and images of each patient was all approved in the ethical committees.

(1) In the first scenario, a patient had a solitary peripheral nonsmall cell lung cancer at the right lung and received SBRT as the initial treatment. At the initial treatment day, metastatic right hilar lymph nodes were detected on CT suggesting that the metastatic nodes had grown during the waiting period for the SBRT. In the cancer board, PRI soon after SBRT to the hilar lymph nodes was suggested to be the best treatment option.
(2) In the second scenario, a patient received fractionated 3D conformal radiograph therapy to the right hilar nodes after open biopsy, which had revealed nonsmall cell lung cancer. At the end of 3D conformal radiograph therapy, a solitary peripheral tumor at the right lung was increasing in size, biopsy proved its malignancy, and the patient was recommended to receive radiograph therapy to the peripheral lung tumor.
(3) In the third scenario, a patient with left breast cancer and axillary lymph nodes had received electron therapy for left chest wall and internal mammary lymphatic region, and 3D conformal radiograph therapy for left supraclavicular and axillary lymphatic region after total mastectomy, left axillary dissection, and perioperative chemotherapy. After 20 months, a solitary metastatic left internal mammary lymph node was detected by positron emission tomography. In the cancer board, PRI using proton therapy to the internal mammary lymph node was suggested to be the best treatment option.

We conducted a sensitivity analysis of PRISTIN, referring to the range of α/β listed in the literature and the range of recovery factors calculated from Evans' formula.

3DRTP was Eclipse (Varian) for radiograph therapy and VQA (Hitachi, Tokyo, Japan) for proton therapy. High-energy radiograph/electron therapy machine was TrueBeam (Varian) in all scenarios, and proton therapy machine was PROBEAT-RT (Hitachi, Tokyo, Japan) in the third scenario.

Results

First scenario

The clinical target volume in the first CT (CTV1) for the peripheral primary lung cancer is shown in Fig. 2. Since metastatic hilar lymph nodes were detected on the initial treatment day, the dose to the CTV1 was intentionally lowered than the usual SBRT for peripheral lung cancer. The total absorbed dose to the CTV1 was 44 Gy and the number of fractions was 7 giving $\text{BED}_{\alpha/\beta=10}$=72 Gy, which is equivalent to 60 Gy in 30 fraction (60 Gy/30 Fr) without correction for regrowth in the first plan.

CTV2 in second plan, CTV for the hilar lymph nodes, is shown in Fig. 2 as well. In reirradiation, the physician wanted to give $\text{2ndBED}_{\alpha/\beta=10}$ equivalent to 60 Gy/30 Fr to the CTV2. The $\text{CBED}_{\text{OAR's }\alpha/\beta}$-volume constraints to the right main bronchus were weighted the highest priority followed by $\text{CBED}_{\text{OAR's }\alpha/\beta}$-volume constraints to the whole lung parenchyma. The tolerable maximum $\text{CBED}_{\alpha/\beta=2}$ for the main bronchus and trachea was assumed to be

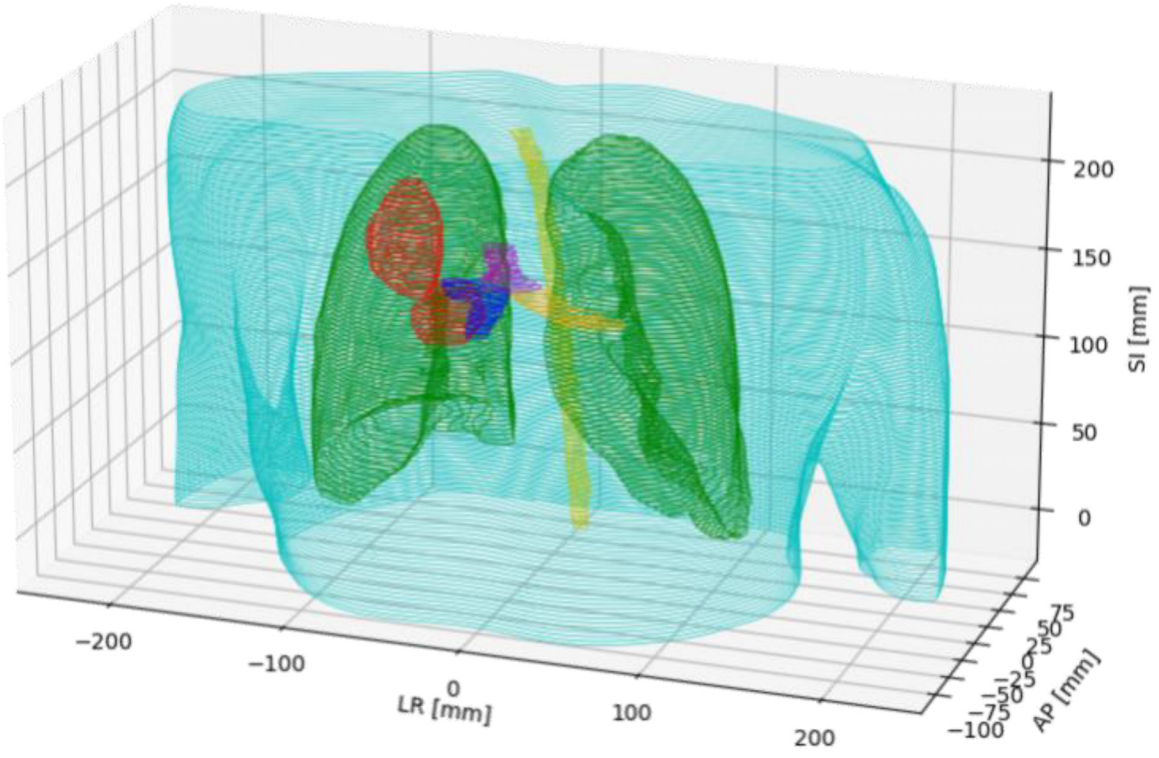

Figure 2 Positional relationship between each organ and target volumes used in scenario 1 and also in scenario 2. The gross tumor volume and clinical target volume at the peripheral right lung field and those at the right hilum are shown in red. Right main bronchus, left main bronchus, trachea, lung, and spinal cord are shown in blue, orange, magenta, green, and yellow. AP = antero-posterior; LR = left-right.

157 Gy, which is equivalent to 74 Gy/33 Fr, based on the treatment protocol in the Novel Approach to Radiotherapy in Locally Advanced Lung cancer 2 (NARLAL2) study.[27] The tolerable volume of $CBED_{\alpha/\beta=2}$>60 Gy, which is equivalent to $CBED_{\alpha/\beta=2}$>20 Gy/5 Fr, was assumed to be 4 cm^3, which is close to the treatment protocol in NRG Oncology/RTOG 0813 Trial.[28] The tolerable mean $CBED_{\alpha/\beta=2}$ for the whole lung parenchyma excluding gross tumor volume (GTV) was assumed to be 26 Gy, which is equivalent to 20 Gy/33 Fr used in NARLAL2, lower than 18 Gy/4 Fr in JCOG0403,[29] and 20 Gy/3 Fr in the RTOG and European Organization for Research and Treatment of Cancer constraints.[30]

In the final second plan, calculated $CBED_{\alpha/\beta=2}$ for each voxel in the right bronchial tree according to the number of fractions (n) from n = 1 to n = 35 is shown in Table 1. Other details of calculated results are shown in Supplementary E4. Using 5 times a week schedule, 22 fractions can be given in 30 days, which is the maximum treatment period in the institutional protocol. PRISTIN suggested that 57.153 Gy/22 Fr is the most appropriate schedule giving $2ndBED_{\alpha/\beta=10}$=72.0 Gy, which is close to 60 Gy/30 Fr. The maximum $CBED_{\alpha/\beta=2}$ to the right main bronchus was 124.078 Gy, which is lower than 157 Gy, tolerable maximum $CBED_{\alpha/\beta=2}$. Table 2 shows the volume for corresponding range of $CBED_{\alpha/\beta=2}$ to the right main bronchus. The total volume that would receive $CBED_{\alpha/\beta=2} \geq$ 60 Gy and ≥100 Gy was 0.833 cm^3 and 0.108 cm^3, respectively, for the right main bronchus. The mean $CBED_{\alpha/\beta=2}$ was 18.332 Gy for the total lung parenchyma excluding GTV, which is lower than 26 Gy, tolerable mean $CBED_{\alpha/\beta=2}$. The maximum $CBED_{\alpha/\beta=2}$ was 5.4 Gy for the trachea. The transaxial distribution of $CBED_{\alpha/\beta=2}$ at the level of tracheal bifurcation is shown in Fig. 3.

Second scenario

In the second scenario, the sequence of the first plan and second plan in the first scenario has been swapped (Fig. 2). In this simulation, the right hilar notal region was the CTV1 and treated using 57.5 Gy in 22 fractions in 30 days as the initial RT. The physician wanted to give $BED_{\alpha/\beta=10}$=72 Gy equivalent to 60 Gy/30 Fr to the CTV2, a solitary peripheral tumor at the right lung by PRI in second plan.

The $CBED_{OAR's\ \alpha/\beta}$-volume constraints to the right main bronchus were weighted the highest priority followed by $CBED_{OAR's\ \alpha/\beta}$-volume constraints to the whole lung parenchyma excluding GTV in the second plan. Supplementary E5 shows relationship among number of fractions, prescribing absorbed dose to the CTV2, and the maximum $CBED_{\alpha/\beta=2}$ in the right bronchus and the mean $CBED_{\alpha/\beta=2}$ to the lung parenchyma excluding

Table 1 Examples of coordinates of the voxels and the $CBED_{\alpha/\beta=2}$ in each voxel in the right bronchial tree for scenario 1

LR	AP	SI	CBED (n=1)	CBED (n=2)	CBED (n=3)	CBED (n=4)	CBED (n=35)
−36	−10	102.5	72.87576	67.75654	64.37207	61.84138	44.1574
−35	−10	102.5	60.11627	56.27985	53.74349	51.84695	38.59434
−34	−10	102.5	48.14387	45.45996	43.68555	42.35876	33.08741
−33	−10	102.5	38.26962	36.48499	35.30511	34.42287	28.25798
−38	−9	102.5	102.1191	93.91623	88.49311	84.43804	56.10201
−37	−9	102.5	83.77277	77.52519	73.39473	70.30623	48.72442
−36	−9	102.5	69.86537	65.0537	61.87256	59.4939	42.87233
−35	−9	102.5	58.94778	55.22654	52.76632	50.92672	38.07198
−34	−9	102.5	48.45405	45.74114	43.94755	42.60642	33.23487
			:				
−25	−8	135	4.49703	4.83865	5.06451	5.23339	6.41352

Abbreviations: AP = antero-posterior; CBED(n = i) = cumulative biological effective dose when the number of fractions is i; LR = left-right; SI = superior-inferior.

GTV. The minimum number of fractions was 7 using 5 times a week in the institutional protocol. PRISTIN suggested that 44.152 Gy/7 Fr is the most appropriate schedule as the final second plan. The maximum $CBED_{\alpha/\beta=2}$ of the right main bronchus was 117.209 Gy at the 7 fractions, which is lower than 157 Gy. The mean $CBED_{\alpha/\beta=2}$ was 17.478 Gy for the total lung parenchyma excluding GTV, which is lower than 26 Gy. The maximum $CBED_{\alpha/\beta=2}$ was 5.4 Gy for the trachea.

Third scenario

The CTV1 in the first plan was left chest wall, supraclavicular, axillary lymphatic region, and internal mammary lymphatic region. The prescription dose was 55 Gy/20 Fr using 5 times a week schedule.

Table 2 $CBED_{\alpha/\beta=2}$-volume statistics for the right main bronchus in scenario 1

$CBED_{\alpha/\beta=2}$ (Gy)	Cumulative voxels	Cumulative (cm^3)
120≦	4	0.010
110≦	13	0.033
100≦	43	0.108
90≦	84	0.210
80≦	129	0.323
70≦	226	0.565
60≦	333	0.833
50≦	489	1.223

Abbreviation: CBED = cumulative biological effective dose.
The voxel size was 1 × 1 × 2.5 mm.

In the second plan, CTV2 was the metastatic left internal mammary lymph node. $CBED_{OAR's\ \alpha/\beta}$-volume constraints to the aorta were weighted the highest priority followed by $CBED_{OAR's\ \alpha/\beta}$-volume constraints to the whole lung parenchyma excluding GTV. The tolerable maximum $CBED_{\alpha/\beta=2}$ for the aorta was assumed to be 157 Gy based on the treatment protocol in NARLAL2 study,[27] which is equivalent to 74 Gy/33 Fr, and lower than 268 Gy(47 Gy/5 Fr) in the NRG Oncology/RTOG 0813 Trial.[28] On the institutional protocol for proton therapy, the maximum treatment time period was 42 days using 5 times a week schedule. The physician wanted to give $2ndBED_{\alpha/\beta=10}$ as much as possible to the CTV2.

PRISTIN suggested that 71.675 Gy/30 Fr is the most appropriate schedule for the CTV2 using proton therapy (Fig. 4). The maximum $CBED_{\alpha/\beta=2}$ was 145.796 Gy for the aorta, which is lower than 157 Gy, tolerable maximum $CBED_{\alpha/\beta=2}$. The total volume of the aorta which would receive $CBED_{\alpha/\beta=2} > 100$ Gy was 0.800 cm^3 (Supplementary E6).

The sensitivity of the PRISTIN to the difference in the α/β ratio and recovery factor of OARs was shown in Supplementary E7 for 3 scenarios. The appropriate number of fractions suggested by PRISTIN did not change for the α/β ratio from 0.1 to 6 for serial organs, 0.1 to 8.5 for parallel organ, and recovery factor from 0 to 0.65 in all scenarios.

Discussion

While several existing tools for reirradiation planning offer automated or semiautomated workflows for dose accumulation and plan optimization, these systems are often limited by reliance on simple summation methods,

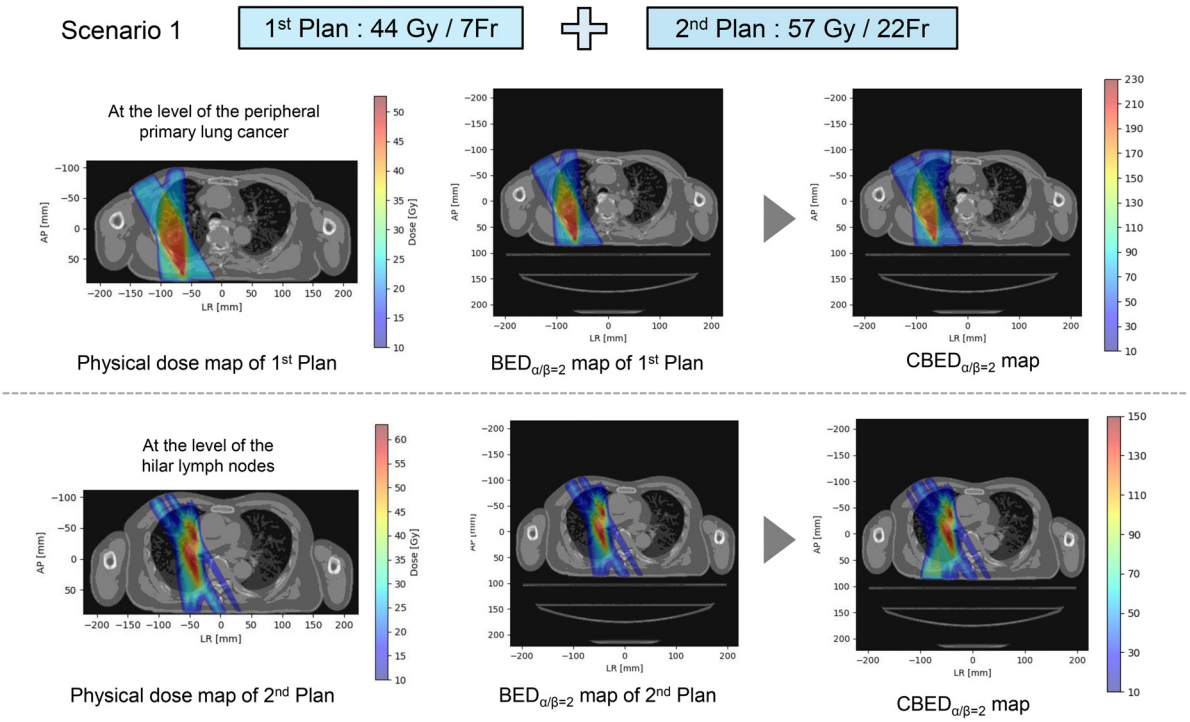

Figure 3 The absorbed dose, BED$_{\alpha/\beta=2}$ map for the first plan (initial radiation therapy) and second plan (PRI), and CBED$_{\alpha/\beta=2}$ map on transaxial images using PRISTIN in scenario 1. The color scales for absorbed dose maps are different from those for BED$_{\alpha/\beta=2}$/CBED$_{\alpha/\beta=2}$ maps. The upper 3 images are on the transaxial CT images at the level of the peripheral primary lung cancer and the lower 3 images are at the level of the hilar lymph nodes.
Abbreviation: BED = biological effective dose; CBED = cumulative biological effective dose; CT = computed tomography.

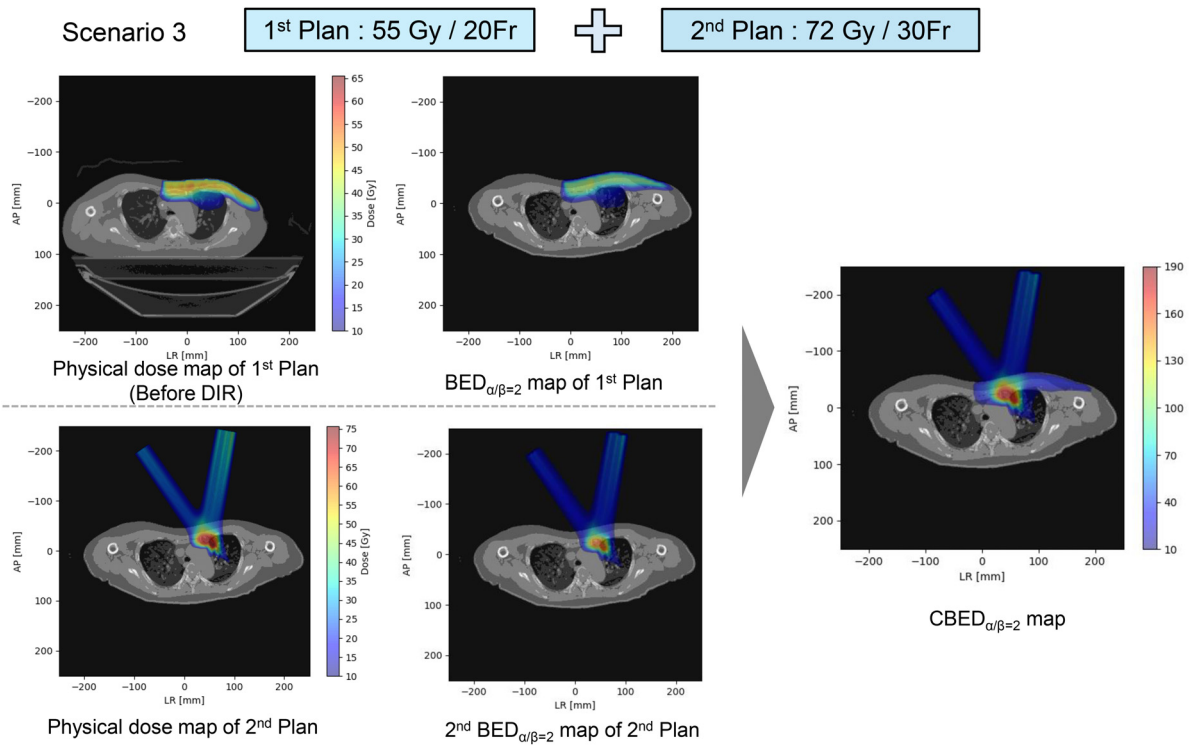

Figure 4 The absorbed dose, BED$_{\alpha/\beta=2}$ map for the first plan (initial electron therapy) and second plan (proton therapy), and CBED$_{\alpha/\beta=2}$ maps on transaxial CT images using PRISTIN in scenario 3. The color scales for absorbed dose maps are different from those for BED$_{\alpha/\beta=2}$/CBED$_{\alpha/\beta=2}$ maps. The absorbed dose map of first plan overlapped on the CT scan before deformable image registration (DIR).
Abbreviation: BED = biological effective dose; CBED = cumulative biological effective dose; CT = computed tomography.

fixed daily dose, or lack of individualized radiobiological modeling. In contrast, PRISTIN uniquely provides voxel-based CBED evaluation, optimization of both prescribing absorbed dose and number of fractions, and individualized α/β and recovery modeling for each OAR and tumor. Furthermore, PRISTIN applies rational constraints based on organ structure (the mean CBED for parallel organs, the maximum CBED for serial), enabling a more biologically accurate and patient-specific approach. These features distinguish PRISTIN from existing tools and support its potential to improve plan quality and reduce toxicity risk in clinical practice. Flowchart of the treatment planning tool for reirradiation in our study is similar to the tool reported by Murray et al[18] and García-Alvarez et al.[17] These tools including the present tool are usable only when DIR is considered reliable for voxel-by-voxel calculation of cumulative dose mapping. Also, the stepwise process to find the prescription dose in reirradiation by using the cumulative biologically equivalent dose is similar. However, both studies did not show how to select the number of fractions after the selection of $EQD2_{\text{tumor's }\alpha/\beta}$ for the target. Since the $EQD2_{\text{OAR's }\alpha/\beta}$ in each voxel in OARs is not proportional to the $EQD2_{\text{tumor's }\alpha/\beta}$ for the target and changes with the daily dose, their workflows are insufficient when daily dose is not the same between initial RT and reirradiation. Accordingly, they fixed the daily dose for reirradiation, same as the initial RT throughout the workflow.

The workflow in the present study is suitable for reirradiation when the most appropriate number of fractions needs to be determined in addition to the prescribing absorbed dose to the target in reirradiation. Compared to previously reported workflows, no additional biological hypothesis and free parameters are required so that they can also implement our findings in their system. The workflow shown by Murray et al[18] has the advantage of optimizing plans with objective functions in EQD2 with the background dose distribution in 3DRTP, possibly after correction for recovery, which was not available in the present study. As García-Alvarez et al[17] did, the same daily dose in first plan is required to be used as the starting point to make second plan in the 3DRTP in the present study. However, this study shows that the appropriate number of fractions and prescribing absorbed dose was successfully calculated afterward using PRISTIN in each scenario.

In previous studies, the maximum of cumulative $EQD2_{\text{OAR's }\alpha/\beta}$ of the OARs was used as the $CBED_{\text{OAR's }\alpha/\beta}$-volume constraints.[17,18] In the present study, the maximum $CBED_{\text{OAR's }\alpha/\beta}$ is only used for serial OAR, which is a reasonable assumption in general. However, as is well known, the maximum $CBED_{\text{OAR's }\alpha/\beta}$ is not a reasonable constraint for parallel OAR.[31] The present study showed that the mean $CBED_{\text{OAR's }\alpha/\beta}$ is the reasonable $CBED_{\text{OAR's }\alpha/\beta}$-volume constraints for parallel OAR theoretically in PRI (Supplementary E3). This is an important general finding for reirradiation suggesting that any supporting tool for reirradiation can use the mean $CBED_{\text{OAR's }\alpha/\beta}$ as the constraint for parallel OAR.

In the previous studies about the mathematical method for selecting a hypofractionation or multiple fractionation regimen based on absorbed dose distribution and biological consideration, it has been shown that (1) there is potential for hypofractionation to be selected even if the OAR is more sensitive to fractionation than the tumor, and (2) there is an interdependence between the spatial dose distribution and the optimal fractionation schedule.[20,21,32] Several papers have explored the nonuniform spatiotemporal fractionation (STF) to the target volume to improve therapeutic ratio.[22,23,33-38] The present PRISTIN is, in fact, regarded as the tool for nonuniform STF to the OARs as well. If you assume that the second plan is used soon after first plan for the same patient, the combination of first plan and second plan is regarded as a nonuniform STF. PRI is, in fact, a kind of nonuniform spatiotemporally fractionated RT, in which a part of body is treated earlier using the fractionation in first plan and another part of body is treated later using different fractionation in second plan.

Our results showed that $CBED_{\text{OAR's }\alpha/\beta}$ of right main bronchus was smaller in hypofractionation than multiple fractionations in scenario 2 (Supplementary E5). Although the difference was small in this example, it is notable that hypofractionation decreased, not increased, the $CBED_{\text{OAR's }\alpha/\beta}$ of the right main bronchus. Generally speaking, because $CBED_{\text{OAR's }\alpha/\beta}$ can be much closer to the tolerable $CBED_{\text{OAR's }\alpha/\beta}$ in reirradiation than in initial RT, a small increase in $2ndBED_{\text{OAR's }\alpha/\beta}$ can cause significant increase in the late damage of the OAR. Sensitivity study by changing locations of CTV used in this study is required in the future to estimate the uncertainties of the final second plan.

There are several limitations in the present study. At first, in real world, after the initial RT, there must be strong deformation of the normal tissues that affect the preciseness of DIR.[39] In cases of severe postradiation anatomic changes such as fibrosis and volume loss, its limitations may be partially mitigated through rigorous quality assurance, careful algorithm selection, targeted application, advanced imaging techniques, uncertainty quantification, and multidisciplinary review—though achieving reliable results in such complex cases remains difficult.[40] The second limitation is that PRISTIN does not have an ability to optimize the conformity and homogeneity of $2ndBED_{\alpha/\beta=10}$ in the target volume at this moment. The present study is using a reference point in CTV2 for prescription but not considering about the conformity and homogeneity of $2ndBED_{\text{tumor's }\alpha/\beta}$ in CTV2. The change of number of fractions induces the change in the $2ndBED_{\text{tumor's }\alpha/\beta}$ distribution in the target volume with the same absorbed dose distribution. For example, if the reference point of CTV2 is set at the voxel with minimal

dose or D_{99}, the reduction in the number of fractions increases the $2ndBED_{\alpha/\beta=10}$ in some voxels in the target volume. Ödén et al[41] have used absorbed dose, not EQD2, for optimizing the conformity and homogeneity in CTV. Future iterations of PRISTIN will focus on developing and integrating algorithms to optimize $2ndBED_{\alpha/\beta=10}$ distribution for CTV using the concept of STF.[20,42,43] Recent reports have suggested that functions to incorporate positional and model-related uncertainties are useful to improve the robustness of the supporting tool for PRI.[17,19,44] Their suggestions are informative to improve the program in PRISTIN further. The third limitation is that the physician still needs to determine the constraints about the number of fractions, that is, the minimum and maximum number of factions. It is because there is still much uncertainty in tumor biology such as reoxygenation and repopulation. However, recently, prospective studies are increasing to find the appropriate number of fractions for various cancers clinically.[45,46] These investigations would reduce the uncertainty in the biological model and improve the clinical value of PRISTIN in future.

Conclusion

The supporting tool, PRISTIN, was suggested to be useful to find the appropriate absorbed dose to the target as well as the number of fractions for precise reirradiation. Compared to conventional reirradiation planning methods, which rely on empirical or simple summation approaches, the PRISTIN tool enables precise voxel-based evaluation of CBED for each OAR. By optimizing both the prescribing absorbed dose and number of fractions to satisfy organ-specific constraints, PRISTIN facilitates individualized treatment planning and is expected to reduce the risk of severe adverse events. Beyond in-silico validation, our future plans for PRISTIN include retrospective and prospective clinical studies, technical integration with clinical workflows, and multi-institutional trials to rigorously validate its safety, efficacy, and clinical impact before widespread clinical adoption. To further enhance the clinical utility of PRISTIN, the tool could be extended by integrating more advanced radiobiological models—such as those accounting for hypoxia, repopulation, or DNA repair kinetics—and by incorporating patient-specific parameters, enabling individualized predictions of radiation response and toxicity based on genetic, clinical, or imaging biomarkers.

Disclosures

Keiji Kobashi used to be an employee of the research institute of Hitachi Ltd, Japan, till January 2025. Hitachi Ltd has paid for joint research to Hidefumi Aoyama at Hokkaido University.

Acknowledgments

Hiroki Shirato was responsible for statistical analysis.

Declaration of AI and AI-Assisted Technologies in the Writing Process

During the preparation of this work the authors used Perplexity/ Perplexity AI, Inc, in order to improve language and readability. After using this tool/service, the authors reviewed and edited the content as needed and take full responsibility for the content of the publication.

Supplementary materials

Supplementary material associated with this article can be found in the online version at doi:10.1016/j.adro.2025.101904.

References

1. Christ SM, Ahmadsei M, Wilke L, et al. Long-term cancer survivors treated with multiple courses of repeat radiation therapy. *Radiat Oncol*. 2021;16:208.
2. Choi JI, Khan AJ, Powell SN, et al. Proton reirradiation for recurrent or new primary breast cancer in the setting of prior breast irradiation. *Radiother Oncol*. 2021;165:142-151.
3. Fattahi S, Ahmed SK, Park SS, et al. Reirradiation for locoregional recurrent breast cancer. *Adv Radiat Oncol*. 2021;6:100640.
4. LaRiviere MJ, Dreyfuss A, Taunk NK, Freedman GM. Proton reirradiation for locoregionally recurrent breast cancer. *Adv Radiat Oncol*. 2021;6:100710.
5. Chakraborty MA, Khan AJ, Cahlon O, et al. Proton reirradiation for high-risk recurrent or new primary breast cancer. *Cancers (Basel)*. 2023;15:5722.
6. De Ruysscher D, Faivre-Finn C, Le Pechoux C, Peeters S, Belderbos J. High-dose re-irradiation following radical radiotherapy for non-small-cell lung cancer. *Lancet Oncol*. 2014;15:e620-e624.
7. Willmann J, Appelt AL, Balermpas P, et al. Re-irradiation in clinical practice: Results of an international patterns of care survey within the framework of the ESTRO-EORTC E^2-RADIatE platform. *Radiother Oncol*. 2023;189:109947.
8. Andratschke N, Willmann J, Appelt AL, et al. European society for radiotherapy and oncology and european organisation for research and treatment of cancer consensus on re-irradiation: Definition, reporting, and clinical decision making. *Lancet Oncol*. 2022;23:e469-e478.
9. Lee SF, Hoskin PJ. Re-irradiation practice and ESTRO/EORTC consensus recommendations: 2023 ASTRO education panel. *Ann Palliat Med*. 2024;13:1150-1153.
10. Yamazaki H, Ogita M, Himei K, et al. Carotid blowout syndrome in pharyngeal cancer patients treated by hypofractionated stereotactic re-irradiation using cyberknife: A multi-institutional matched-cohort analysis. *Radiother Oncol*. 2015;115:67-71.
11. You R, Liu YP, Xie YL, et al. Hyperfractionation compared with standard fractionation in intensity-modulated radiotherapy for patients with locally advanced recurrent nasopharyngeal carcinoma: A multicentre, randomised, open-label, phase 3 trial. *Lancet*. 2023;401:917-927.

12. Thorpe CS, Niska JR, Girardo ME, et al. Proton beam therapy reirradiation for breast cancer: Multi-institutional prospective PCG registry analysis. *Breast J*. 2019;25:1160-1170.
13. Chao HH, Berman AT, Simone CB, et al. Multi-institutional prospective study of reirradiation with proton beam radiotherapy for locoregionally recurrent non-small cell lung cancer. *J Thorac Oncol*. 2017;12:281-292.
14. Hardcastle N, Vasquez Osorio E, Jackson A, et al. Multi-centre evaluation of variation in cumulative dose assessment in reirradiation scenarios. *Radiother Oncol*. 2024;194:110184.
15. Paradis KC, Matuszak MM. The medical physics management of reirradiation patients. *Semin Radiat Oncol*. 2020;30:204-211.
16. Vasquez Osorio E, Mayo C, Jackson A, Appelt A. Challenges of reirradiation: A call to arms for physicists - and radiotherapy vendors. *Radiother Oncol*. 2023;182:109585.
17. García-Alvarez JA, Paulson E, Kainz K, et al. Radiobiologically equivalent deformable dose mapping for re-irradiation planning: Implementation, robustness, and dosimetric benefits. *Radiother Oncol*. 2025;205:110741.
18. Murray L, Thompson C, Pagett C, et al. Treatment plan optimisation for reirradiation. *Radiother Oncol*. 2023;182:109545.
19. Mechalakos JG, Hu YC, Kuo L, et al. Radiotherapy dose accumulation routine (radar)—A novel dose accumulation script with built-in uncertainty. *Pract Radiat Oncol*. 2025;15:187-195.
20. Mizuta M, Takao S, Date H, et al. A mathematical study to select fractionation regimen based on physical dose distribution and the linear-quadratic model. *Int J Radiat Oncol Biol Phys*. 2012;84:829-833.
21. Sugano Y, Mizuta M, Takao S, et al. Optimization of the fractionated irradiation scheme considering physical doses to tumor and organ at risk based on dose-volume histograms. *Med Phys*. 2015;42:6203-6210.
22. Unkelbach J, Craft D, Salari E, Ramakrishnan J, Bortfeld T. The dependence of optimal fractionation schemes on the spatial dose distribution. *Phys Med Biol*. 2013;58:159-167.
23. Torelli N, Papp D, Unkelbach J. Spatiotemporal fractionation schemes for stereotactic radiosurgery of multiple brain metastases. *Med Phys*. 2023;50:5095-5114.
24. Unkelbach J, Papp D, Gaddy MR, et al. Spatiotemporal fractionation schemes for liver stereotactic body radiotherapy. *Radiother Oncol*. 2017;125:357-364.
25. van Leeuwen CM, Oei AL, Crezee J, et al. The alfa and beta of tumours: A review of parameters of the linear-quadratic model, derived from clinical radiotherapy studies. *Radiat Oncol*. 2018;13:96.
26. Quashie EE, Li XA, Prior P, et al. Obtaining organ-specific radiobiological parameters from clinical data for radiation therapy planning of head and neck cancers. *Phys Med Biol*. 2023;68:24.
27. Thomsen SN, Møller DS, Knap MM, et al. Daily CBCT-based dose calculations for enhancing the safety of dose-escalation in lung cancer radiotherapy. *Radiother Oncol*. 2024;200:110506.
28. Bezjak A, Paulus R, Gaspar LE, et al. Safety and efficacy of a five-fraction stereotactic body radiotherapy schedule for centrally located non-small-cell lung cancer: NRG Oncology/RTOG 0813 trial. *J Clin Oncol*. 2019;37:1316-1325.
29. Nagata Y, Hiraoka M, Shibata T, et al. Prospective trial of stereotactic body radiation therapy for both operable and inoperable T1N0M0 non-small cell lung cancer: Japan Clinical Oncology Group study jcog0403. *Int J Radiat Oncol Biol Phys*. 2015;93:989-996.
30. Kong FM, Ritter T, Quint DJ, et al. Consideration of dose limits for organs at risk of thoracic radiotherapy: Atlas for lung, proximal bronchial tree, esophagus, spinal cord, ribs, and brachial plexus. *Int J Radiat Oncol Biol Phys*. 2011;81:1442-1457.
31. Seppenwoolde Y, Lebesque JV, de Jaeger K, et al. Comparing different NTCP models that predict the incidence of radiation pneumonitis. Normal tissue complication probability. *Int J Radiat Oncol Biol Phys*. 2003;55:724-735.
32. Mizuta M, Date H, Takao S, et al. Graphical representation of the effects on tumor and oar for determining the appropriate fractionation regimen in radiation therapy planning. *Med Phys*. 2012;39:6791-6795.
33. Unkelbach J, Papp D. The emergence of nonuniform spatiotemporal fractionation schemes within the standard bed model. *Med Phys*. 2015;42:2234-2241.
34. Unkelbach J, Bussière MR, Chapman PH, Loeffler JS, Shih HA. Spatiotemporal fractionation schemes for irradiating large cerebral arteriovenous malformations. *Int J Radiat Oncol Biol Phys*. 2016;95:1067-1074.
35. Kim M, Phillips MH. A feasibility study of spatiotemporally integrated radiotherapy using the LQ model. *Phys Med Biol*. 2018;63:245016.
36. Kim M, Stewart RD, Phillips MH. A feasibility study: Selection of a personalized radiotherapy fractionation schedule using spatiotemporal optimization. *Med Phys*. 2015;42:6671-6678.
37. Adibi A, Salari E. Spatiotemporal radiotherapy planning using a global optimization approach. *Phys Med Biol*. 2018;63:035040.
38. Fujarewicz K, Lakomiec K. Adjoint sensitivity analysis of a tumor growth model and its application to spatiotemporal radiotherapy optimization. *Math Biosci Eng*. 2016;13:1131-1142.
39. Regnery S, Leiner L, Buchele C, et al. Comparison of different dose accumulation strategies to estimate organ doses after stereotactic magnetic resonance-guided adaptive radiotherapy. *Radiat Oncol*. 2023;18:92.
40. Nenoff L, Amstutz F, Murr M, et al. Review and recommendations on deformable image registration uncertainties for radiotherapy applications. *Phys Med Biol*. 2023;68:24TR01.
41. Ödén J, Eriksson K, Svensson S, et al. Technical note: Optimization functions for re-irradiation treatment planning. *Med Phys*. 2024;51:476-484.
42. Unkelbach J, Zeng C, Engelsman M. Simultaneous optimization of dose distributions and fractionation schemes in particle radiotherapy. *Med Phys*. 2013;40:091702.
43. Torelli N, Unkelbach J. Fraction-variant beam orientation optimization for spatiotemporal fractionation schemes. *Med Phys*. 2025;52:4723-4741.
44. Thompson C, Pagett C, Lilley J, et al. Brain re-irradiation robustly accounting for previously delivered dose. *Cancers (Basel)*. 2023;15:3831.
45. Gensheimer MF, Gee H, Shirato H, et al. Individualized stereotactic ablative radiotherapy for lung tumors: The ISABR phase 2 nonrandomized controlled trial. *JAMA Oncol*. 2023;9:1525-1534.
46. Liu F, Farris MK, Ververs JD, Hughes RT, Munley MT. Histology-driven hypofractionated radiation therapy schemes for early-stage lung adenocarcinoma and squamous cell carcinoma. *Radiother Oncol*. 2024;195:110257.